Modified Costas Signal

NADAV LEVANON, Fellow, IEEE
ELI MOZESON
Tel Aviv University
Israel

A modification to the Costas signal is suggested. It involves an increase of the frequency separation Δf beyond the inverse of the subpulse duration t_b, combined with adding linear FM (LFM) with bandwidth B, in each subpulse. Specific relationships between Δf and B will prevent autocorrelation grating lobes, that would normally appear when $t_b \Delta f > 1$.

Manuscript received May 4, 2003; revised November 6, 2003 and April 27, 2004; released for publication April 27, 2004.

IEEE Log No. T-AES/40/3/835890.

Refereeing of this contribution was handled by P. Lombardo.

Authors' address: Dept. of Electrical Engineering–Systems, Tel Aviv University, POB 39040, Tel Aviv, 69978, Israel, E-mail: (nadav@eng.tau.ac.il).

0018-9251/04/$17.00 © 2004 IEEE

I. INTRODUCTION

A Costas array [1] is an $N \times N$ binary array, filled with N "ones" and $N(N-1)$ "zeros." There is exactly one "1" in each row and in each column. The two-dimensional discrete autocorrelation function (ACF) of the array should exhibit only "1" and "0" values, except at the origin where the autocorrelation value is N. Construction algorithms for Costas arrays appear in [2].

In a Costas signal the N rows of the array represent N frequencies spaced Δf apart, and the N columns represent N contiguous subpulses ("bits"), each of duration t_b. A 1 in the (i,j) element of the array indicates that during the jth time interval the ith frequency is transmitted. A Costas signal dictates a specific relationship between the frequency spacing and the bit duration

$$\Delta f = \frac{1}{t_b}. \tag{1}$$

This crucial relationship results in orthogonality between the different frequencies, when the integration time is equal to t_b. Due to the orthogonality, the ACF of the complex envelope of the Costas signal exhibits nulls at all multiples of t_b. It will also result in nulls at all but $N(N+1)+1$ grid points of the ambiguity function (AF), when the grid spacings are Δf and t_b. (In addition to the origin, where the AF value is 1, at each delay nt_b, $n = \pm 1, \pm 2, \ldots, \pm(N-1)$ there are, respectively, $N - |n|$ Doppler gird points with non-zero AF value. Namely, there are $2[1 + 2 + \cdots + (N-1)] = N(N+1)$ grid points with AF value of exactly $1/N$.) The pulse compression ratio of a Costas signal is N^2. Namely, the first ACF null is found at $\tau = T/N^2 = t_b/N$, where T is the total pulse duration.

Lower frequency spacing ($\Delta f < 1/t_b$) degrades the delay resolution. The ACF mainlobe widens and the ACF nulls disappear. Higher frequency spacing ($\Delta f > 1/t_b$) narrows the ACF mainlobe (because the signal bandwidth has increased) but results in additional high ACF peaks within the delay interval $-t_b < \tau < t_b$, known as "grating lobes." We show later (see (7)) that when

$$\Delta f = a/t_b, \qquad a > 1 \tag{2}$$

the grating lobe(s) appear at

$$\tau_g = \pm g \frac{t_b}{a}, \qquad g = 1, 2, \ldots, \lfloor a \rfloor \tag{3}$$

where $\lfloor a \rfloor$ indicates the largest integer smaller than a. The AF and ACF of a Costas signal in which $N = 8$ and $\Delta f = 5/t_b$ are shown in Figs. 1 and 2. The grating lobes (four on each side of the mainlobe) are clearly evident in both figures.

The frequency evolution of the signal is plotted in Fig. 3. The bandwidth, normalized with respect to the

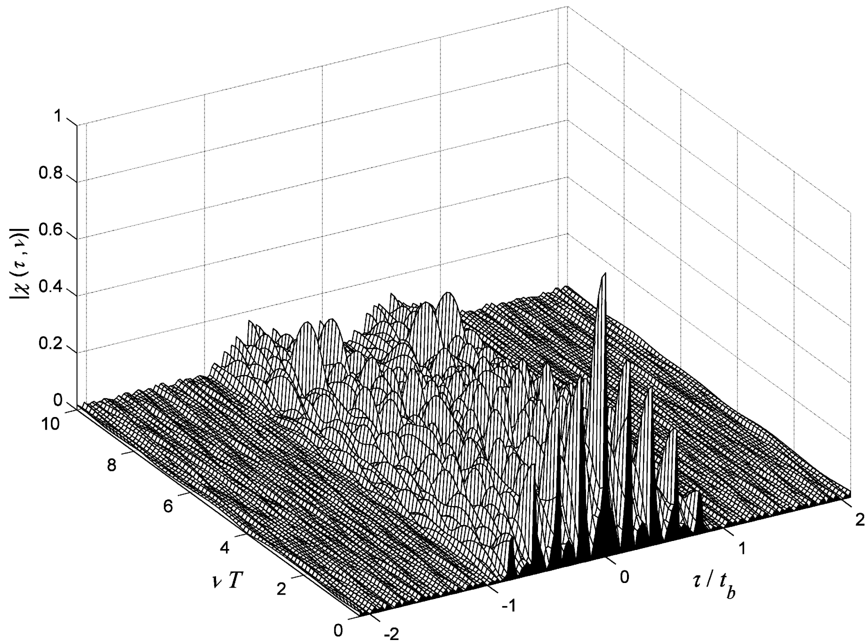

Fig. 1. AF of Costas signal with $N = 8$, $\Delta f = 5/t_b$, (zoom on $|\tau| \le 2t_b = T/4$).

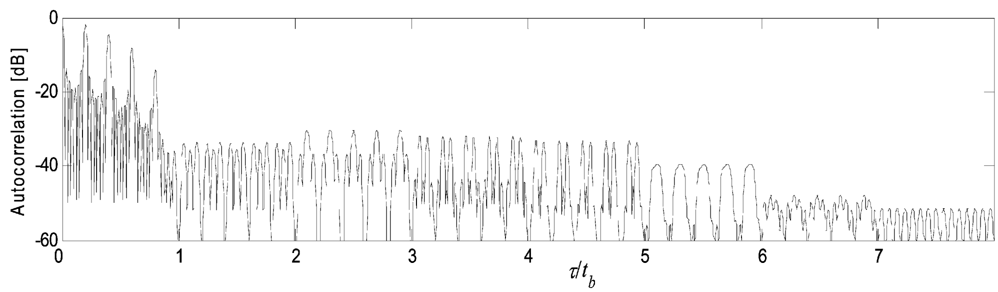

Fig. 2. ACF (dB) of Costas signal with $N = 8$, $\Delta f = 5/t_b$.

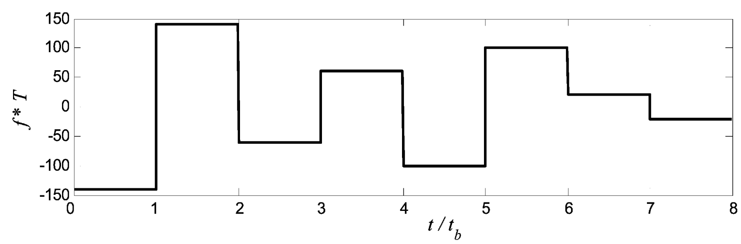

Fig. 3. Frequency evolution of Costas signal with $N = 8$, $\Delta f = 5/t_b$.

entire signal duration T, is given by

$$T\left[(f_{\max}) - f_{\min}) + \frac{1}{t_b}\right] = N(N-1)t_b\Delta f + N = 8 \cdot 7 \cdot 5 + 8 = 288. \tag{4}$$

This product is the time-bandwidth product (TBW) of the signal, which is approximately its compression ratio. Note that the TBW (= 288), achieved because of the larger frequency spacing, is much higher than the TBW (= 64) of a regular Costas signal of length 8. The penalty is the grating lobes. The next section shows how the grating lobes can be nullified while maintaining the large frequency spacing, hence the large bandwidth.

II. ADDING INTRABIT LFM NULLIFIES THE GRATING LOBES

The problem of grating lobes is encountered in a popular radar signal known as a train of stepped-frequency pulses. In that signal large overall bandwidth is achieved gradually by frequency stepping unmodulated pulses separated in time. In stepped-frequency train of unmodulated pulses,

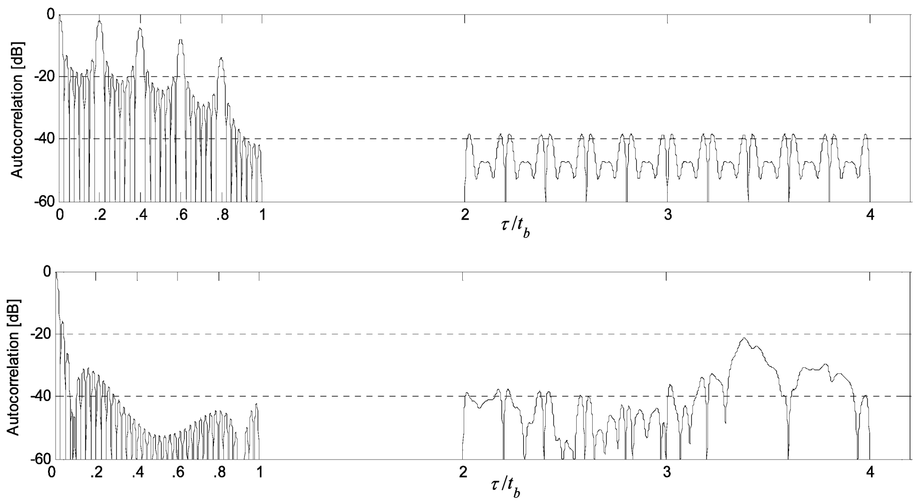

Fig. 4. ACF of a train of 8 stepped-frequency pulses ($T_r/t_b = 3$, $t_b\Delta f = 5$). Costas frequency order: 1 8 3 6 2 7 5 4. Top: $t_bB = 0$. Bottom: $t_bB = 12.5$.

ACF grating lobes appear when the product of the pulsewidth times the frequency step exceeds one. Replacing the fixed-frequency pulses with linear FM (LFM) pulses [3] was used to attenuate grating lobes (as well as sidelobes). In a recent paper [4] an analytic expression of the AF of such a stepped-frequency train of N LFM pulses was derived for delay τ within the individual pulse duration, assigned the symbol t_b. The AF expression is valid as long as the pulse repetition interval T_r obeys $T_r > 2t_b$. The zero-Doppler cut of the AF, which is the magnitude of the ACF, within the mainlobe area ($|\tau| \le t_b$), turns out to be a product of two expressions

$$\left|R\left(\frac{\tau}{t_b}\right)\right| = \left|R_1\left(\frac{\tau}{t_b}\right)\right|\left|R_2\left(\frac{\tau}{t_b}\right)\right|, \qquad \left|\frac{\tau}{t_b}\right| \le 1. \quad (5)$$

The first is due to a single LFM pulse with bandwidth B,

$$\left|R_1\left(\frac{\tau}{t_b}\right)\right| = \left|\left(1-\left|\frac{\tau}{t_b}\right|\right)\operatorname{sinc}\left[TB\frac{\tau}{t_b}\left(1-\left|\frac{\tau}{t_b}\right|\right)\right]\right|, \qquad \left|\frac{\tau}{t_b}\right| \le 1. \quad (6)$$

The second term describes the grating lobes,

$$\left|R_2\left(\frac{\tau}{t_b}\right)\right| = \left|\frac{\sin\left(N\pi t_b\Delta f\frac{\tau}{t_b}\right)}{N\sin\left(\pi t_b\Delta f\frac{\tau}{t_b}\right)}\right|, \qquad \left|\frac{\tau}{t_b}\right| \le 1. \quad (7)$$

Clearly $|R_2(\tau/t_b)|$ exhibits peaks (mainlobe and grating lobes) at

$$\frac{\tau_{\text{lobes}}}{t_b} = \frac{g}{t_b\Delta f}, \qquad g = 0, \pm1, \pm2, \ldots, \lfloor t_b\Delta f\rfloor, \quad |\tau| < t_b. \quad (8)$$

TABLE I
Examples of Valid Cases

m	n	$t_b\Delta f$	t_bB	$B/\Delta f$
1	0	2	4	2
1	1	3	4.5	1.5
2	2	3	9	3
2	3	5	12.5	2.5
3	3	3	13.5	4.5
3	4	4	16	4
4	4	3	18	6
4	5	3.667	20.1667	5.5
5	6	3.5	24.5	7
4	7	9	40.5	4.5

Nullifying the grating lobes is based on requiring that the nulls of $|R_1(\tau/t_b)|$ coincide with the grating lobes of $|R_2(\tau/t_b)|$. In [4] that requirement was shown to imply the following relationships

$$t_b\Delta f = \frac{4m-n}{2m-n} \quad (9)$$

$$t_bB = \frac{(4m-n)^2}{2(2m-n)} \quad (10)$$

where m and n are integers. Some examples, in which all the grating lobes are nullified, are given in Table I.

The ACF expression in (5) is independent of the order in which the pulses are arranged in time. Hence, arranging the pulses in a Costas sequence maintains the nullifying. Equation (5) is also independent of the pulse repetition interval T_r, as long as it is larger than twice the pulse duration, namely $T_r > 2t_b$. An example of the ACF of a train of 8 separated stepped-frequency pulses, with and without LFM, is given in Fig. 4. The delay axis extends as far as the first recurrent lobe, in order to show the significant difference between the ACF mainlobe area and the recurrent lobe area.

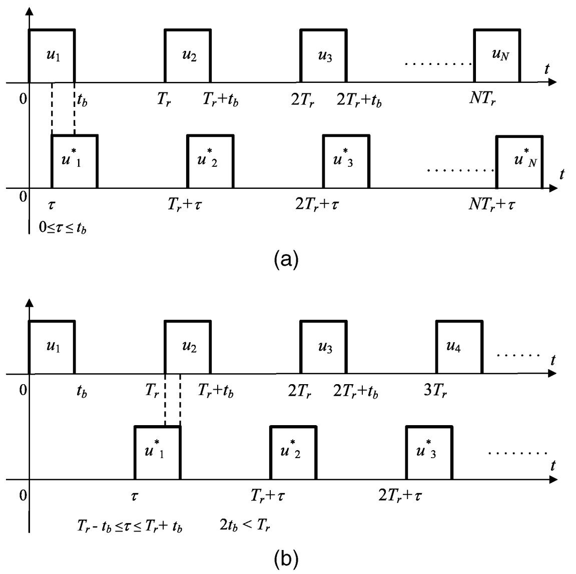

Fig. 5. Alignment of signal and reference pulses when calculating: (a) mainlobe area of ACF, (b) first ACF recurrent lobe area.

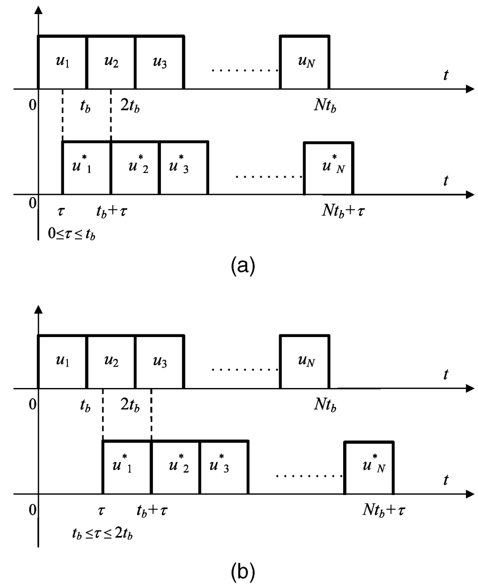

Fig. 6. Alignment of signal and reference Costas subpulses when calculating: (a) first bit area of the ACF, (b) second bit area.

Fig. 5 demonstrates schematically the different alignments of the received and reference pulses yielding the mainlobe area of the ACF (pair a), and yielding the first ACF recurrent lobe (pair b). Regarding the ACF mainlobe area we can write

$$R(\tau) = \sum_{p=1}^{N} R_{u_p u_p}(\tau), \qquad 0 \le \tau \le t_b \tag{11}$$

where

$$R_{u_p u_p}(\tau) = \int_0^{t_b} u_p(t) u_p^*(t+\tau)\,dt, \qquad 0 \le \tau \le t_b. \tag{12}$$

The exact expression of ACF outlined in (11) was given in (5), (6), and (7).

When calculating the first recurrent lobe area of the ACF, cross terms are involved

$$R(\tau) = \sum_{p=2}^{N} R_{u_p u_{p-1}}(\tau). \tag{13}$$

Because the complex envelopes $u_p(t)$ of different pulses have different center frequencies, the spectral overlap is relatively small, yielding ACF recurrent lobes that are considerably lower than the mainlobe. In addition to showing the lower recurrent lobe, Fig. 4 also shows the disappearance of the grating lobes within the mainlobe area ($|\tau| \le t_b$), when LFM with a specific $t_b B$ product was added.

III. CONVERTING THE TRAIN OF SEPARATED PULSES INTO CONTIGUOUS SUBPULSES

Converting the train of separated pulses into contiguous subpulses ($T_r = t_b$) changes the ACF expression. The new alignment of pulses (now subpulses) is demonstrated in Fig. 6. The changes in the ACF over $|\tau| \le t_b$ (where the grating lobes are found) are additional terms due to the cross correlation between adjacent subpulses,

$$R(\tau) = \sum_{p=1}^{N} R_{u_p u_p}(\tau) + \sum_{p=2}^{N} R_{u_p u_{p-1}}(\tau), \qquad 0 \le \tau \le t_b. \tag{14}$$

At higher delays ($t_b < |\tau|$) only cross terms are found in the ACF.

Note that the dominant contribution to the ACF in (14) is the first sum. Exactly the same sum was found when the pulses were separated, and its expression was given in (5)–(7). That first sum may exhibit ACF grating lobes (without LFM), or they may be nullified if the proper LFM is added. That sum is not affected by the polarity of the LFM slope of the individual subpulses.

The additional sum of cross terms does depend on the polarity of the LFM slope of the individual subpulses. When the slope polarity is the same in all subpulses, the cross terms involving adjacent bits, and for positive delays $\tau < t_b$, were found to be

$$|R_{u_p u_{p-1}}(\tau)| = \left| \frac{\sin\left[\pi t_b \left((k_p - k_{p-1})\Delta f + B\dfrac{\tau - t_b}{t_b} \right) \dfrac{\tau}{t_b}\right]}{\pi t_b \left((k_p - k_{p-1})\Delta f + B\dfrac{\tau - t_b}{t_b} \right)} \right|, \qquad 0 \le \tau \le t_b \tag{15}$$

where k_p is an integer and $k_p \Delta f$ is the carrier frequency of the pth subpulse.

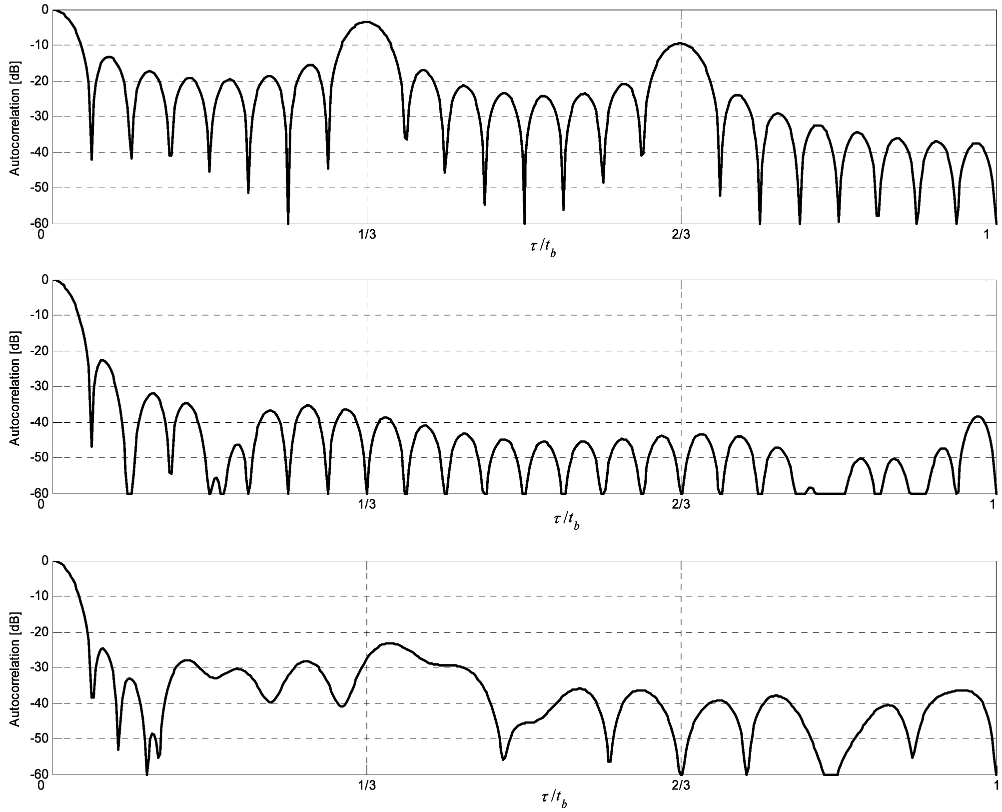

Fig. 7. ACF of train of 8 stepped-frequency pulses, Costas order: 1 8 3 6 2 7 5 4, ($t_b\Delta f = 3$). Top: $T_r/t_b = 3$, $t_bB = 0$. Middle: $T_r/t_b = 3$, $t_bB = 13.5$. Bottom: $T_r/t_b = 1$, $t_bB = 13.5$.

In order to check if the nullifying holds we should be interested in the value of (15) at the position of the grating lobes, namely at $\tau = r/\Delta f$, where r is an integer smaller than $t_b\Delta f$. Since r is an integer and $k_p - k_{p-1}$ is an integer, (15) can be reduced to

$$\left|R_{u_p u_{p-1}}\left(\frac{r}{\Delta f}\right)\right| = \left|\frac{\sin\left[\frac{\pi B r}{\Delta f}\left(\frac{r}{t_b\Delta f} - 1\right)\right]}{\pi t_b\left[(k_p - k_{p-1})\Delta f + B\frac{r}{t_b\Delta f} - B\right]}\right|. \tag{16}$$

The numerator of (16) is zero if and only if (IFF) the argument of the sine function is an integer multiple of π. Using the values of t_bB and $t_b\Delta f$ that were given in (9) and (10) gives the argument of the sine function (after division by π) as

$$\frac{r}{2}[r(2m - n) - 4m + n] = m(r-2)r - \frac{n(r-1)r}{2} \tag{17}$$

which is always integer since $r(r-1)$ is even for all r. Thus the numerator of (16) will be zero whenever t_bB and $t_b\Delta f$ nullify the original grating lobes. The only case where the entire fraction in (16) will not equal zero is when the denominator is also zero, resulting in $\sin(0)/0$. Thus if

$$\begin{aligned}(k_p - k_{p-1}) &+ \frac{B}{\Delta f}\left(\frac{r}{t_b\Delta f} - 1\right)\\ &= (k_p - k_{p-1}) + \frac{4m-n}{2}\left[\frac{r}{4m-m}(2m-n) - 1\right]\\ &= (k_p - k_{p-1}) + m(r-2) - \frac{n(r-1)}{2} = 0\end{aligned} \tag{18}$$

for some r, m, n, and $(k_p - k_{p-1})$, the corresponding rth grating lobe will not be nullified. For the Costas sequence 1 8 3 6 2 7 5 4, out of all the cases in Table I, only three will loose some or all the nulls. For example in the case $m = 3$, $n = 3$, $k_4 - k_3 = 6 - 3 = 3$, the $r = 1$ null will be lost. This example is demonstrated in Fig. 7, which plots the ACF of the first bit.

For the top part of Fig. 7 the pulses are separated, and there is no LFM. The two ACF grating lobes, caused by using ($t_b\Delta f = 3$), are clearly evident. For the middle part, the pulses remained separated but an appropriate LFM was added. The resulted nullifying of the grating lobes is clearly evident. For the bottom part the spacing between the pulses was closed, converting them into a single modified Costas pulse. The second grating lobe at $\tau/t_b = 2/3$ remained nullified, however the null corresponding

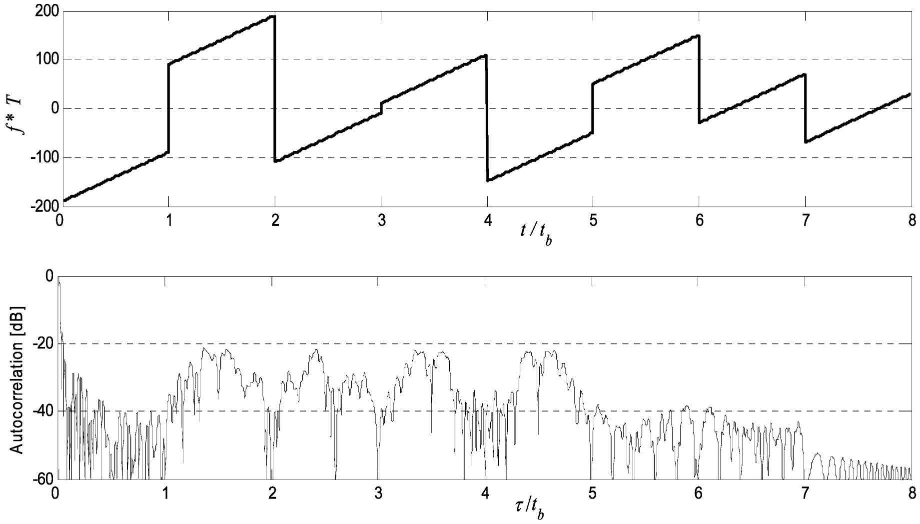

Fig. 8. Frequency evolution (top) and ACF (bottom) of 8 element modified Costas pulse, Costas frequency order: 1 8 3 6 2 7 5 4, $t_b B = 12.5$, $t_b \Delta f = 5$, fixed slope polarity.

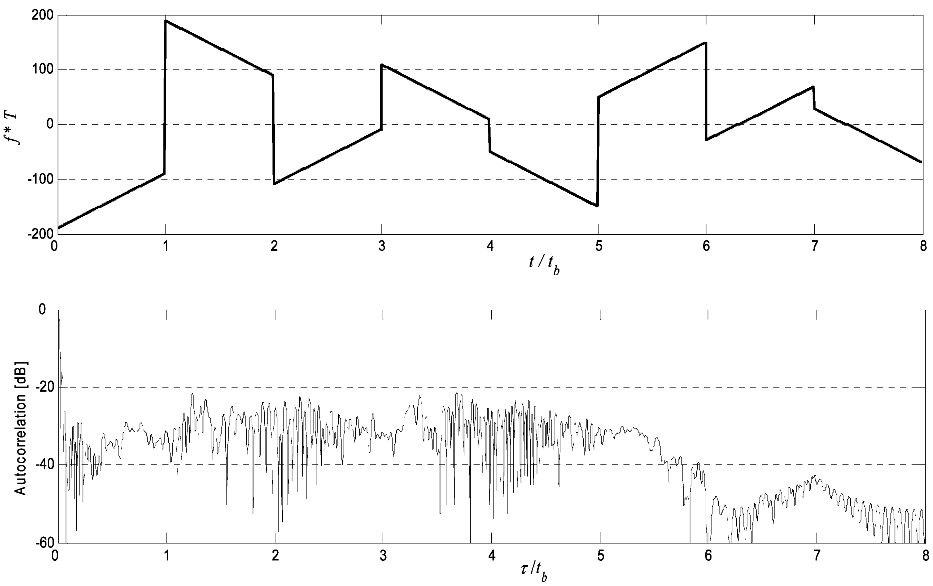

Fig. 9. Frequency evolution (top) and ACF (bottom) of 8 element modified Costas pulse, Costas frequency order: 1 8 3 6 2 7 5 4, $t_b B = 12.5$, $t_b \Delta f = 5$, alternating slope polarity.

to the first grating lobe was lost, as predicted in the preceding paragraph. Yet, while the original grating lobe at $\tau/t_b = 1/3$ was -3.5 dB (top subplot), the new value at that delay is approximately -28 dB (bottom subplot). Comparing the middle and bottom subplots of Fig. 7 shows that the transition from separated pulses to contiguous subpulses increased the ACF sidelobes somewhat, but kept them below -22 dB.

We can conclude that loosing a null at a particular $\tau = r/\Delta f$ does not imply that the grating lobe was restored. It only implies that the ACF value at that delay is no more identically zero. Because of the relatively weak contribution from the cross terms, the ACF value will remain very low (typically below -20 dB). This is true for the case of equal slope polarity (for which the analytic expression in (15) was found) as well as for the case of alternating slope polarity, for which we do not have an analytic expression.

In Figs. 8 and 9 we present the frequency evolution and the resulted ACF for modified Costas pulses of length 8, when the slope polarity is fixed (Fig. 8) or alternating (Fig. 9).

An appealing intuitive rule for deciding which of the subpulses should have an inverted frequency slope, says that subpulses at adjacent frequency slots (not necessarily adjacent time slots) should have opposite frequency slopes, because the spectral overlap between such pairs is the largest. This is the alternating rule used in Fig. 9.

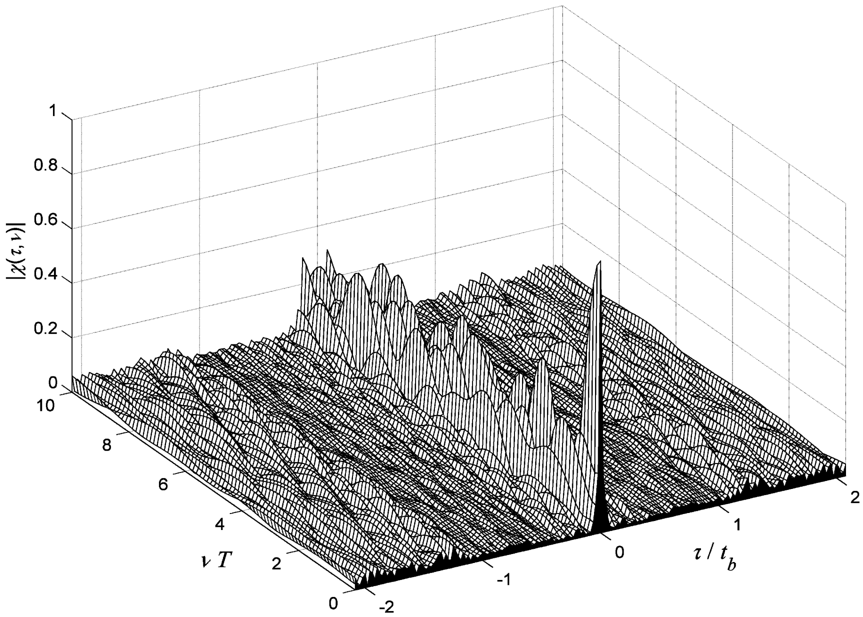

Fig. 10. AF of modified Costas signal with $N = 8$, $t_b \Delta f = 5$, $t_b B = 12.5$, zoom on $|\tau| \le 2t_b = T/4$.

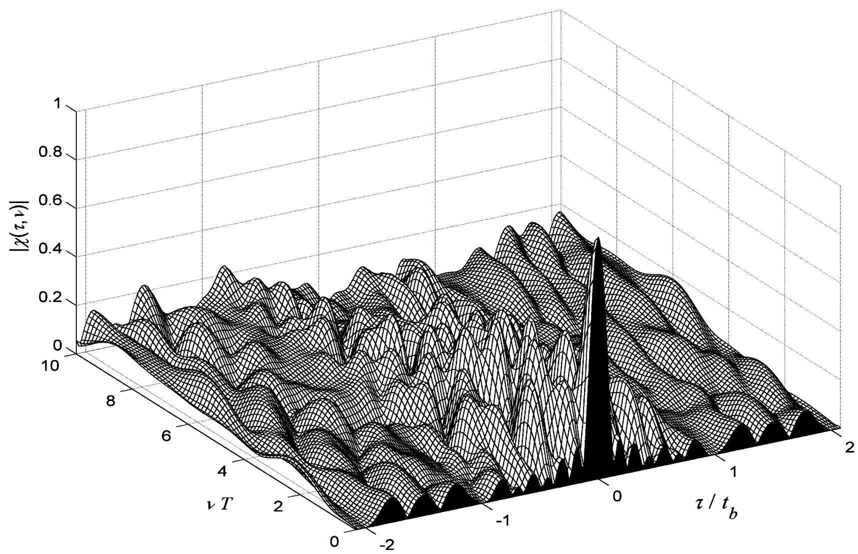

Fig. 11. AF of classical Costas signal with $N = 8$, $t_b \Delta f = 1$, $t_b B = 0$, zoom on $|\tau| \le 2t_b = T/4$.

The peak-to-peak frequency deviation, multiplied by the total pulse duration T, is given by

$$\begin{aligned} T(f_{\max} - f_{\min}) &= \frac{T}{t_b}[(N-1)t_b \Delta f + t_b B] \\ &= N[(N-1)t_b \Delta f + t_b B]. \qquad (19) \end{aligned}$$

This product is approximately the TBW of the signal, and also its time compression ratio. For the example given in Figs. 8 or 9 (in which $N = 8$) the above equation yields $T(f_{\max} - f_{\min}) = 380$. A conventional Costas signal needs 19 or 20 ($\approx \sqrt{380}$) elements to get a similar compression ratio.

So far we presented ACF plots of the modified Costas signal. In order to demonstrate how well the ACF nulls (or reduction) hold for higher Doppler shifts we present in Fig. 10 the partial AF (delay zoom on the first two bits, out of eight) of the signal shown in Fig. 9. This plot should be compared with Fig. 1 (same $t_b \Delta f$ but no LFM), and with Fig. 11 which presents the AF of a classical 8 element Costas signal, in which $t_b \Delta f = 1$.

IV. CONCLUSIONS

Adding LFM to the individual subpulses of a Costas signal allows an increase in the frequency spacing Δf much beyond the $1/t_b$ spacing dictated in a conventional Costas signal. The resulted increase in bandwidth improves the delay resolution, which otherwise would have required a considerably longer Costas sequence (by a factor of $\sqrt{t_b \Delta f}$, if the total signal duration is unchanged). Maintaining one of several possible relationships between the frequency spacing and the LFM bandwidth will prevent ACF grating lobes, which would have appeared if LFM was not added. The suggested modified Costas signal could be useful in situations where adding LFM is easier than increasing the length of the Costas sequence.

REFERENCES

[1] Costas, J. P. (1984)
A study of a class of detection waveforms having nearly ideal range-Doppler ambiguity properties.
Proceedings of the IEEE, **72**, 8 (1984), 996–1009.

[2] Golomb, S. W., and Taylor, H. (1984)
Construction and properties of Costas arrays.
Proceedings of the IEEE, **72**, 9 (1984), 1143–1163.

[3] Rabideau, D. J. (2002)
Nonlinear synthetic wideband waveforms.
In *Proceedings of the IEEE Radar Conference*, Los Angeles, CA, May 2002, 212–219.

[4] Levanon, N., and Mozeson, E. (2003)
Nullifying ACF grating lobes in stepped-frequency train of LFM pulses.
IEEE Transactions on Aerospace and Electronic Systems, **39**, 2 (Apr. 2003), 694–703.

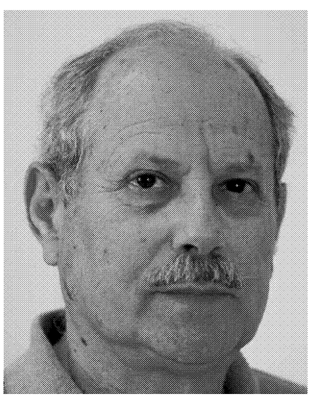

Nadav Levanon (S'67—M'70—SM'83'—F'98) received a B.Sc. and M.Sc. degrees from the Technion–Israel Institute of Technology, in 1961 and 1965, and a Ph.D. from the University of Wisconsin–Madison, in 1969, all in electrical engineering.

He has been a faculty member at Tel Aviv University since 1970, where he is a professor in the Department of Electrical Engineering–Systems. He was chairman of the EE-Systems Department during 1983–1985. He spent sabbatical years at the University of Wisconsin, The Johns Hopkins University–Applied Physics Lab., and Qualcomm Inc., San Diego, CA.

Dr. Levanon is a member of the ION and AGU and a Fellow of the IEE. He is the author of the book *Radar Principles* (Wiley, 1988) and coauthor of *Radar Signals* (Wiley, 2004).

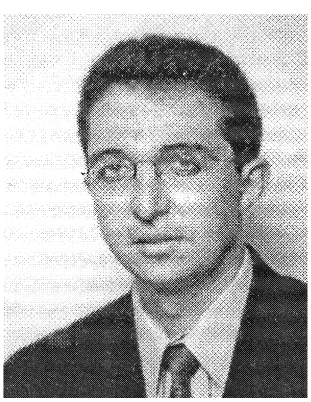

Eli Mozeson was born in 1970. He received his B.Sc., M.Sc. and Ph.D. degrees from Tel Aviv University in 1992, 1999, and 2003, all in electrical engineering.

Since 1992 he serves in the Israeli Air Force as an electronic engineer.

Dr. Mozeson is coauthor of the book *Radar Signals* (Wiley, 2004).